International Journal of Heat and Mass Transfer 80 (2015) 72–84

Contents lists available at ScienceDirect

International Journal of Heat and Mass Transfer

journal homepage: www.elsevier.com/locate/ijhmt

Large eddy simulations of turbulent circular wall jets

Shuai Zhang [a], Adrian Wing-Keung Law [a,*], Bing Zhao [a]

[a] School of Civil and Environmental Engineering, and DHI-NTU Centre, NEWRI, Nanyang Technological University, 50 Nanyang Avenue, Singapore 639798, Singapore

ARTICLE INFO

Article history:
Received 4 April 2014
Received in revised form 24 July 2014
Accepted 30 August 2014
Available online 27 September 2014

Keywords:
LES
Wall jets
Velocity distribution
Scalar mixing characteristics
Turbulence intensity

ABSTRACT

Turbulent circular wall jets have been extensively investigated both experimentally and numerically in the past decades. Most of the previous studies focus on the kinematic characteristics of the jet flows, while the mixing characteristics including the scalar transport have not been well examined. The current study performs a comprehensive investigation of the turbulent circular wall jet including both the flow and mixing characteristics using the large eddy simulations (LES) approach with proper near-wall modelling. The LES results are compared to the existing experimental measurements, as well as numerical results from two other Reynolds-averaged Navier–Stokes (RANS) models: the standard k-ε and standard k–ω models, with enhanced wall functions. The comparison focuses on the velocity and scalar distributions, rates of velocity and scalar decay, variations of characteristic length scales, and turbulence intensities in different directions. Overall, the study shows that LES coupling with proper near-wall modelling can simulate both the kinematic and mixing characteristics of the turbulent wall jet in a satisfactory manner, and the accuracy is superior to the RANS models with enhanced wall functions for this three-dimensional wall-bounded shear flow. The advantages can be attributed directly to the better simulations of the anisotropic jet spreading near the wall.

1. Introduction

The occurrence of turbulent circular jets is common in many industrial applications. For a free circular jet, the jet flow expands in an axisymmetrical manner. However, when the jet is placed next to an impermeable wall, i.e. a turbulent wall jet, the flow becomes asymmetrical due to the no flux condition at the wall. There are extensive applications of turbulent wall jets in the industry, such as film-cooling of the wall of a turbine [1] and effluent discharges into shallow water where the effluent port is located near the bottom [2].

Turbulent circular wall jets have been well studied experimentally in the past few decades. Sforza and Herbst [3] performed laboratory measurements on the three-dimensional turbulent wall jet. The results showed that the growth of the mixing layer is independent of the nozzle shape, which only affects the decay rate of maximum velocity near the nozzle. Rajaratnam and Pani [4] investigated the velocity distribution within the turbulent wall jet. They revealed that the vertical cross-sectional velocity distribution includes two different flow regions: (a) below the maximum velocity as the boundary layer, and (b) above the maximum velocity as the free mixing region. Moreover, they observed the similarity of velocity profiles in both streamwise and spanwise directions in the Zone of Established Flow, and that the lateral spreading rate is 4–5 times larger than normal spreading rate. Launder and Rodi [1] reviewed the literature and also conducted experimental investigations on the flow behaviour of wall jets. Padmanabham and Gowda [5] quantified the mean flow characteristics of three-dimensional wall jets experimentally using the technique of the total pressure probe. Law and Herlina [6] performed a comprehensive experimental study on the turbulent circular wall jet including both kinematic and scalar mixing characteristics. They observed that the velocity spreading rate is consistent with the data of Rajaratnam and Pani [4], but the concentration spreading rate is nearly 1.5 times higher while the wall normal to lateral concentration spreading ratio is approximately equal to 5 for both. In addition to the mean flow behaviour, the turbulence characteristics of the circular wall jet, including the distribution of the turbulent mass transport, were also investigated by Herlina and Law [7]. More experimental investigations on turbulent wall jets had also been performed by Abrahamsson et al. [8], Gerodimos and So [9], and Eriksson et al. [10].

Computational studies on turbulent wall jets had also been performed in the past. Craft and Launder [11] numerically simulated the three-dimensional turbulent wall jet with Reynolds Averaged Navier Stokes (RANS) models and several turbulence closures. They confirmed that the remarkably higher lateral spreading rate is due

* Corresponding author. Tel.: +65 6790 5296.
E-mail address: cwklaw@ntu.edu.sg (A.W.-K. Law).

http://dx.doi.org/10.1016/j.ijheatmasstransfer.2014.08.082
0017-9310/

to the creation of streamwise vorticity, rather than asymmetric diffusion. However, the lateral spreading rate in Craft and Launder's [11] simulations was about 50% higher than most of the experimental measurements. Lubcke et al. [12] also investigated the spreading mechanism of three-dimensional turbulent wall jets using RANS models. They demonstrated that the Boussinesq viscosity model failed to reproduce the lateral spreading mechanism. Dejoan and Leschziner [13] explored the mean flow and turbulence characteristics of a plane turbulent wall jet by large eddy simulations (LES). Li et al. [14] adopted LES to examine the flow and dilution behaviour of an axisymmetric jet imparting the wall perpendicularly. Subsequently, Li et al. [15] also simulated numerically the kinematic characteristics of the circular wall jet, but the scalar characteristics were not examined.

The previous numerical studies on three dimensional turbulent wall jets focused only on the kinematic characteristics, while the mixing behaviour or scalar transport had not been addressed so far. The understanding of the scalar transport of the circular wall jet is important for the engineering assessment discussed above, and it also contributes towards the fundamental understanding of wall bounded shear flows. In this study, we employ LES with proper near-wall modelling to evaluate both the kinematic and scalar mixing characteristics of the turbulent circular wall jet. Based on the results, we shall demonstrate that the performance of LES in simulating the three-dimensional turbulent wall jet with proper near-wall modelling is satisfactory. The LES results are also superior to the results from RANS models with enhanced wall functions. In the following, we shall first introduce the various numerical approaches. The numerical results are then presented and compared to the available data in the literature. The key findings are given at the end.

2. Computational methodology

2.1. Governing equations

The governing equations, including the continuity and momentum equations, for a three-dimensional, incompressible fluid flow are as follow [16]:

Continuity equation:

$$\frac{\partial u_i}{\partial x_i} = 0 \tag{1}$$

Momentum equation:

$$\frac{\partial}{\partial t}(\rho u_i) + \frac{\partial}{\partial x_j}(\rho u_i u_j) = -\frac{\partial p}{\partial x_i} + \frac{\partial}{\partial x_j}\left(\mu \frac{\partial u_i}{\partial x_j}\right) + \frac{\partial \tau_{ij}}{\partial x_j} \tag{2}$$

Scalar transport equation:

$$\frac{\partial}{\partial t}(\rho \phi) + \frac{\partial}{\partial x_j}(\rho \phi u_j) = \frac{\partial}{\partial x_j}\left(\Gamma \frac{\partial \phi}{\partial x_j}\right) + \frac{\partial Q_j}{\partial x_j} \tag{3}$$

where u_i, u_j are the mean velocity in i, j direction, respectively; ρ is the fluid density; p is the pressure, μ is the fluid viscosity, t is the time, Γ is the molecular diffusivity, ϕ is the mean scalar concentration, $\tau_{ij} = -\rho\overline{u_i' u_j'}$ are the Reynolds stresses and $Q_j = -\rho\overline{\phi' u_j'}$ are the turbulent scalar flux, where the apostrophe indicates an instantaneous deviation while the overbar indicates time averaged variables. In the present study, the distribution of scalar concentration is tracked through the variation of a small temperature difference as tracer. Therefore, ϕ is identical to the mean temperature difference. From the equations, it is obvious that the Reynolds stresses and turbulent scalar flux are required to be resolved for the closure of the equations.

With RANS models, the Boussinesq hypothesis is adopted to quantify the Reynolds stresses and the turbulent scalar flux in the following manner:

$$\tau_{ij} = \mu_t\left(\frac{\partial u_i}{\partial x_j} + \frac{\partial u_j}{\partial x_i}\right) - \frac{2}{3}\left(\rho k + \mu_t \frac{\partial u_k}{\partial u_k}\right)\delta_{ij} \tag{4}$$

$$Q_j = \Gamma_t \frac{\partial \phi}{\partial x_j} \tag{5}$$

where μ_t is the eddy viscosity, k is the turbulent kinetic energy and Γ_t is the turbulent dispersivity. The transport equations of the k–ε and k–ω models for μ_t and k are summarised in the Appendix A.

LES approaches the simulations in a different manner. With LES, eddies are filtered into large and small sizes based on the local grid sizes. The large eddies are then computed directly by solving the instantaneous N–S equations, while the small eddies are modelled based on the Boussinesq hypothesis [16]. After the filtering operation, the sub-grid scale (SGS) continuity and momentum equations follow Eqs. (1) and (2) , and the SGS Reynolds stresses are modelled by

$$-\tau_{ij} - \frac{1}{3}\tau_{kk}\delta_{ij} = -2\mu_t \bar{S}_{ij} \tag{6}$$

$$Q_j = \frac{\mu_t}{Pr_t}\frac{\partial \phi}{\partial x_j} \tag{7}$$

where $\tau_{ij} = -\rho\overline{u_i' u_j'} + \rho\overline{u_i' u_j'}$ is the SGS Reynolds stress, μ_t is the SGS eddy viscosity, τ_{kk} is the isotropic part of SGS stress which can be neglected for incompressible flows [17], $Q_j = -\rho\overline{\phi' u_j'} + \rho\overline{\phi' u_j'}$ is the SGS turbulent scalar flux, $Pr_t = 0.85$ is the SGS Prandtl number and $\bar{S}_{ij} = \frac{1}{2}\left(\frac{\partial \bar{u}_i}{\partial u_j} + \frac{\partial \bar{u}_j}{\partial u_i}\right)$ is the rate of strain tensor for the resolved scale.

The major variable that needs to be resolved for LES is the SGS eddy viscosity, μ_t. Various SGS models have been developed in the past, and their details are also briefly summarised in the Appendix A. In turbulent conditions, the transports of mass, momentum, energy, and other quantities are mainly affected by the large eddies which are strongly determined by the geometries and boundary conditions of the flow involved. On the contrary, the small eddies tend to be isotropic and are not as affected by boundaries, thus the turbulent models based on Boussinesq hypothesis are more suitable. Therefore, through the direct simulations of large eddies, LES is expected to yield better predictions of the wall-bounded flows than the RANS models.

In the present study, two standard RANS models (standard k–ε and standard k–ω) and LES with the Smagorinsky SGS model were adopted in the simulations of the three-dimensional wall jet.

2.2. Flow configuration and computational setup

The simulation domain was configured based on the experimental setup in Law and Herlina [6] in Cartesian coordinates. As

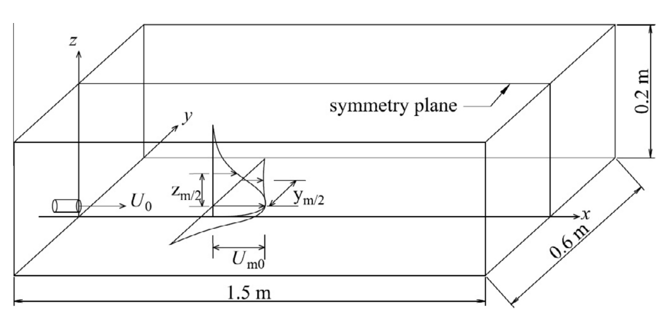

Fig. 1. Schematic diagram of the computational domain.